Observational Study

Medicine®

OPEN

Evaluation of $^{99m}T_C$-ECD SPECT/CT brain Imaging with NeuroGam analysis in Moyamoya disease after surgical revascularization

Jingjing Lou, MD[a,b], Zhuang Liu, MD[a], Bin Xu, MD, PhD[c], Yuan-Kai Wang, MD[a], Cong-Jin Liu, MD[a], Miao Liu, MD[a], Xing-Dang Liu, MD, PhD[a,*]

Abstract

To evaluate the clinical value of NeuroGam software in assessing the brain foci perfusion changes by $^{99m}T_C$-ECD single photon emission computed tomography/computed tomography (SPECT/CT) brain imaging in patients with Moyamoya Disease (MMD).

Seventy-two patients with MMD who underwent superficial temporal artery-middle cerebral artery (STA-MCA) bypass combined with encephalo-duro-myo-synangiosis (EDMS) surgical revascularization were included. Baseline and follow-up $^{99m}T_C$-ECD SPECT/CT brain scans were performed on all patients at least twice before and after operation. Pre- and post-SPECT dicom images were reoriented into Talairach space using NeuroGam Software package. Additional visual analysis was performed. Differences mean pixel value between pre- and post- operation brain perfusion were assessed with paired t test and McNemar test.

Significant differences in the number of hypoperfusion foci were found between visual assessment and NeuroGam aided assessment. More hypoperfusion foci were found by NeuroGam software aided assessment in the frontal, parietal, temporal, occipital lobe, thalamus, basal ganglia and cerebellum before and after surgery ($P < .0001$). According to NeuroGam software assessment, the perfusion of frontal, parietal, temporal lobe, anterior and middle cerebral regions on the operative side significantly improved before and after surgery ($t = -3.734$, $t = -3.935$, $t = -5.099$, $t = -4.006$, $t = -5.170$, all $P < .001$). However, no significant differences were found in the occipital lobe ($t = -1.962$, $P = .054$), thalamus ($t = 1.362$, $P = .177$), basal ganglia ($t = -2.394$, $P = .019$), and cerebellum ($t = 1.383$, $P = .171$) before and after surgery.

The NeuroGam software provides a quantitative approach for monitoring surgical effect of MMD in a variable time (3–12 months after surgery). It could discover the perfusion changes that are neglected in conventional visual assessment.

Abbreviations: AC = anterior Commissure, CCH = crossed cerebellar hypoperfusion, CT = computed tomography, CTP = CT perfusion, DSA = digital subtraction angiography, EDMS = encephalo-duro-myo-synangiosis, ICA = internal carotid artery, MMD = Moyamoya Disease, MRI = magnetic resonance imaging, MRP = MR perfusion, PC = posterior Commissure, PET = positron emission tomography, rCBF = regional cerebral blood flow, $rCMRO_2$ = regional cerebral metabolic rate of oxygen, rOEF = regional oxygen extraction fraction, MTT = mean transit time, ROI = region of interest, SPECT/CT = single photon emission computed tomography/computed tomography, STA-MCA = superficial temporal artery-middle cerebral artery, TCD = transcranial Doppler.

Keywords: $^{99m}T_C$-ECD SPECT/CT brain imaging, Moyamoya disease, NeuroGam, quantification cerebral revascularization

1. Introduction

Moyamoya disease (MMD) is an uncommon idiopathic intracranial vasculopathy characterized by progressive occlusion of the bilateral terminal portion of the internal carotid artery (ICA) and formation of fragile collateral vessels.[1,2] The main symptoms of MMD in most pediatric patients are ischemic attack due to insufficient collateral vessels, while those in adults are usually ischemic attack and/or intracranial bleeding.[3] Owing to the chronic hypoperfusion in frontal lobe, patients may develop intellectual impairment, especially in children.[4] It is generally acknowledged that timely and accurate diagnosis and reasonable treatment are crucial to improve the long-term prognosis of MMD.[5] Revascularization surgery can improve brain perfusion of impaired regions, which seems to be the best choice for MMD patient[6] Therefore, appropriate methods must be found to evaluate patients' cerebral perfusion before and after treatment.[7] Although digital subtraction angiography (DSA) and transcranial Doppler (TCD) could provide the morphologic status of cerebral arteries, both methods are difficult to

Editor: Ismaheel Lawal.

JL and ZL contributed equally to this work.

[a] Department of Nuclear Medicine of Huashan Hospital, Fudan University, [b] Universal Medical Imaging Diagnostic Center, [c] Department of Neurosurgery, Huashan Hospital, Fudan University, Shanghai, China.

[*] Correspondence: Xing-Dang Liu, Department of Nuclear Medicine, Huashan Hospital, Fudan University, 12 Urumqi M. Road, Shanghai, China (e-mail: xingdliu@yahoo.com).

How to cite this article: Lou J, Liu Z, Xu B, Wang YK, Liu CJ, Liu M, Liu XD. Evaluation of 99mTC-ECD SPECT/CT brain Imaging with NeuroGam analysis in Moyamoya disease after surgical revascularization. Medicine 2019;98:46 (e16525).

Received: 24 January 2019 / Received in final form: 25 June 2019 / Accepted: 26 June 2019

http://dx.doi.org/10.1097/MD.0000000000016525

distinguish functional impairment when anatomical changes are inapparent or collateral circulation is not adequately formed. The brain perfusion examinations with voxel-based analysis of $^{99m}T_C$-ECD single photon emission computed tomography/computed tomography (SPECT/CT) may provide a better solution for optimal clinical management of MMD, especially when it comes functional impairment without structural deterioration[8,9] Compared with computed tomography (CT) perfusion (CTP) and magnetic resonance (MR) perfusion (MRP), the result of SPECT brain perfusion seems to be more stable and reliable, on account of its complementary functional information to anatomic imaging examinations.[10] So far, the most common analysis method of SPECT/CT is visual assessment, which is lack of quantitative parameters. Therefore, it may eventually limit the clinical application of SPECT/CT in MMD. Recently, with the development of medical imaging techniques,[11] as well as the improvements of computer-aided procedure,[12] NeuroGam software becomes an efficient tool to observe the perfusion changes. This software can provide quantitative analysis of images and identify the perfusion changes between 2 sequential brain SPECT image of the same patient before and after cerebral revascularization. Furthermore, it can display brain perfusion data through visual inspection as a three-dimensional anatomical topographic representation and show regional differences of cerebral blood flow by a specific color scale.

To the best of our knowledge, few published studies had focused on computer-aided software assessment of cerebral blood changes in patients with MMD. Our study was designed to assess regional differences in cerebral blood flow using $^{99m}T_C$-ECD SPECT/CT combined with NeuroGam software in patients with MMD after superficial temporal artery-middle cerebral artery (STA-MCA) bypass combined with encephalo-duro-myo-synangiosis (EDMS) surgical revascularization.

2. Materials and methods

2.1. Participant

Seventy-two patients with MMD (32 men and 40 women; 40 ± 12 years old, range from 11 to 64 years) were recruited from the Department of Neurosurgery, Huashan Hospital, Fudan University from January 2013 to June 2018. The follow-up time was 3 to 12 months after surgery. All these patients met the diagnostic criteria of MMD, and were confirmed by DSA or CTA according to the guidelines from the Research Committee on Spontaneous Occlusion of the Circle of Willis.[5] And none of the subjects had a history of craniocerebral trauma or major psychopathological conditions.

The selection of patients was decided by a comprehensive evaluation of DSA images, clinical characteristics, and SPECT/CT brain perfusion, and no surgical contraindications were found. They all underwent STA-MCA+EDMS[13] in the involved cerebral hemispheres and the patency of the anastomoses were verified by intraoperative Doppler ultrasound. The first SPECT/CT was performed 3 to 5 days before the operation. The second SPECT/CT was performed 3 to 12 months after operation. Ten healthy controls (6 men and 4 women; 46 ± 16 years old, range from 18–62 years) were enrolled from the regular physical examination center of Huashan hospital and no subject had the history of neurological, psychiatric or certain diseases such as Alzheimer disease, Parkinson disease, epilepsy, depression, schizophrenia and cerebrovascular disease, which may affect brain perfusion. The data obtained from the healthy volunteers provided normal brain perfusion data. And the changes of cerebral perfusion in patients with MMD were analyzed by using it as a standard.

3D Hoffman brain model imaging was performed before SPECT/CT exam for quality control. The study was approved by the Institutional Research and Ethics Committee of Huashan Hospital. Each participant provided informed consent.

2.2. Image acquisition and reconstruction

All adult patients received an intravenous injection of $^{99m}T_C$-bicisate (ethyl cystine dimer [ECD]) 30mCi (1110Mbq; Shanghai GMS Pharmaceutical Co. Ltd.), and for pediatric MMD, a reduced activity of radiopharmaceutical was used. Caffeine and alcohol containing products were avoided 24 hours before examination. After injection, patients rested for 15 minutes with sunglasses in a quiet, dimly lit room to avoid activation of the corresponding cortical areas. And all patients completed the test as required.[14] Whole-brain perfusion images were obtained in all of them. A dual head SPECT/CT (SIEMENS Symbia T16) equipped with a low-energy, high-resolution (LEHR) collimator was used for brain imaging. The head of each patient was held with strips in the head holder.[15] SPECT acquisitions were performed using a 360-degree orbit, matrix size 128×128, ZOOM 1.45, detector automatic form, double-detector acquisition, 128 frames with 360 degree rotation, 5.625 angles per view, and each frame capture 80 k counts. 3D Ordered Subsets Expectation Maximization (OSEM) was used for SPECT image reconstruction (8 subsets and 12 iterations). CT acquisitions was 120 kv tube voltage, 45 mAs, 1.5 mm slice thickness, 256×256 image matrix size, and 110 to 130 slices according to the size of the patients' brain.

2.3. SPECT image analysis

Two experienced nuclear medicine physicians (each has worked for more than 5 years) independently interpreted the SPECT/CT images. They analyzed the differences of cerebral perfusion between left and right hemispheres to find the impaired regions and compared SPECT images with CT images visually. Visual interpretation of the perfusion state was defined in brain ECD uptake in more than 3 continuous slices. They also analyzed the three-dimensional cortical surface data provided by the Neuro-Gam software (Segami Corporation, Siemens Medical Solutions USA, Inc.), which could separate the right and left hemisphere from the right and define outlines of the brain with the vertical Anterior Commissure (AC) line and Posterior Commissure (PC) line. Each image had been quality controlled. After anatomical standardization and voxel normalization, quantifiable perfusion data could be used for comparison. Images were displayed from frontal, transverse and sagittal projections. The processing showed brain perfusion data through visual inspection in a 3D anatomical topographic representation by means of a specific color scale (Fig. 1F).[15] Furthermore, in order to obtain high reproducibility, we selected different lobes, such as frontal, parietal, temporal, occipital lobe, thalamus, basal ganglia and cerebellum, as the region of interest (ROI) and each ROI expressed as corresponding percentage of the entire volume. It also could quantify any perfusion differences of impaired cortices both in severity and size. The quantitative results, including the mean/maximum/minimum pixel value in each corresponding ROI were obtained. The mean pixel value was chosen to quantify the recover levels. For the same patient, we compared the perfusion data before and after surgery.

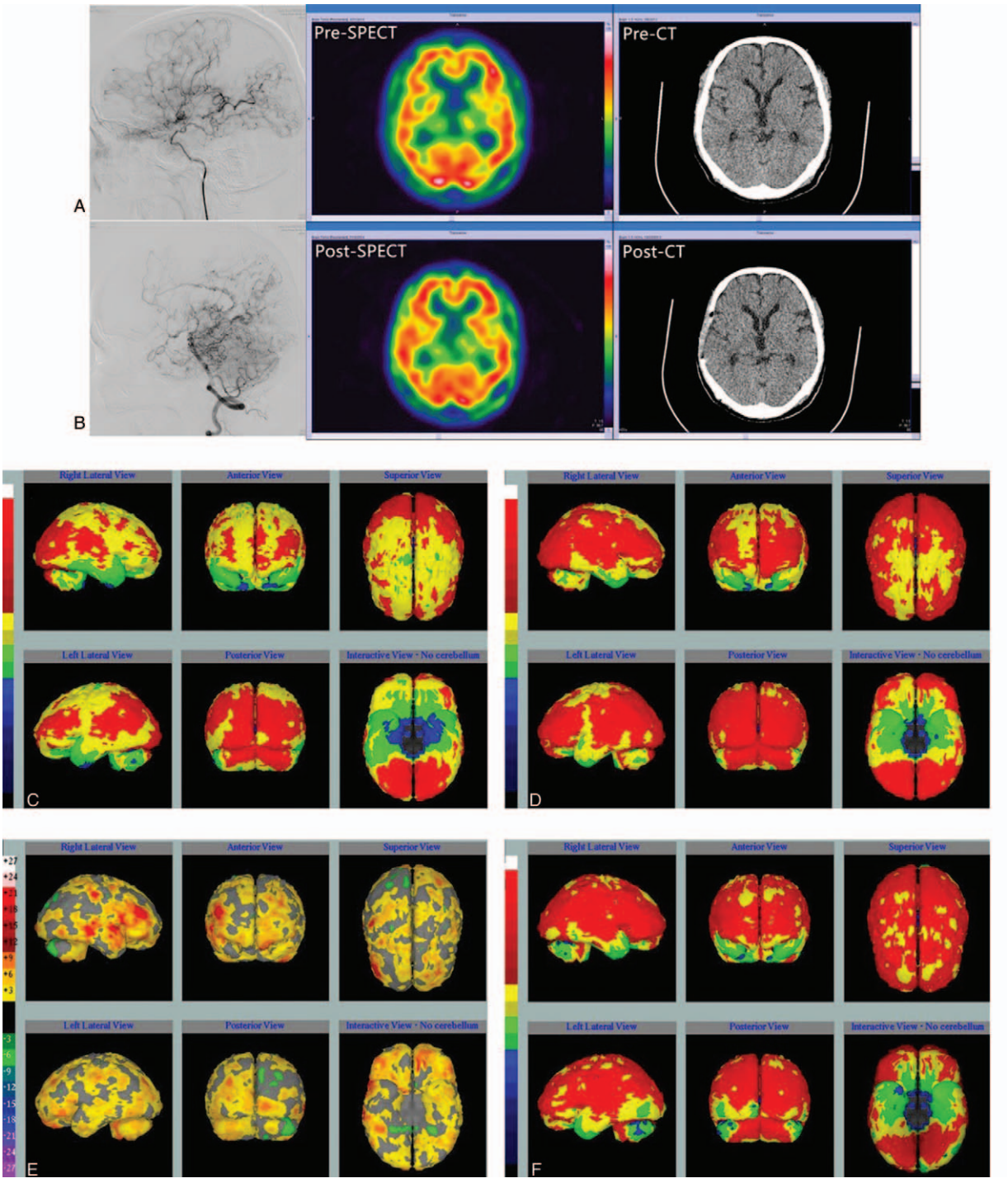

Figure 1. No. 1 patient in Table 1. Male, 41-year-old was admitted to the emergency department for sudden headache with worsening short-term memory and left limb asthenia. CT showed intracranial hemorrhage, and right basal ganglia infarct lesion was also presented. DSA demonstrated bilateral stenosis of both internal carotid arteries and moyamoya vessels. (A-B) Preoperative digital subtraction angiography (DSA) showed occlusion of bilateral terminal portion of the internal carotid artery and moyamoya vessels at the base of the brain. (Pre-SPECT) SPECT showed regions of hypoperfusion in the right frontal lobe and left thalamus. (Pre-CT) Spiral CT scan were unremarkable except foci in basal ganglia of the same slice. Cerebral perfusion study was performed of the same patient with improvement in his symptoms of limb asthenia after the right hemispheres STA-MCA bypass EDMS operation. (Post-SPECT) No change was found in the cerebral perfusion in the right frontal lobe and left thalamus by visual assessment. (Post-CT) Spiral CT showed postoperative changes of the skull besides right basal ganglia infarct lesion. NeuroGam perfusion maps were displayed on 3D images. (C) In this case, there was hypoperfusion in the bilateral frontal and parietal lobes before the operation. (D) The regions of hypoperfusion in the bilateral frontal and parietal lobes decreased after the operation. (E) Brain perfusion in the bilateral frontal, parietal, temporal, and occipital lobes was marked highly than pre-operation, especially in surgical hemisphere (right). (F) Example of a normal 3D cortical surface displayed by NeuroGam software in control group. Color scale on the left of the picture illustrated the brain perfusion station.

2.4. Statistical analysis

For each patient, post-treatment data were compared with pretreatment data. Differences between different groups were assessed by paired *t* test. In addition, Mcnemar test was used to investigate differences between visual and combined NeuroGam assessment. Differences were statistically significant if the *P* value <.05. All statistical analyses were performed using SPSS (v. 16.0.1, Chicago, IL; and Medcalc, Mariakerke, Belgium).

3. Results

Among 72 subjects, intracranial hemorrhages were present in 29 cases, limb asthenia in 41 patients, memory deterioration in 35 patients. Frequent headaches, dizziness or quadrantanopia, aphasia and dysarthria were found in 38 patients, 2 of which had aneurysm. Hypothyroidism was found in one patient. Epilepsies were present in three patients. After the operation, clinical symptoms, especially increased muscle strength, obviously relieved in 32 cases. The majority of MMD patients showed increased brain perfusion after the operation.

Before the MCA-STA bypass EDMS cerebral revascularization, the numbers of hypoperfusion foci in anterior and middle cerebral arteries territories of visual assessment and NeuroGam aided assessment were 50(35%) vs 88(61%), 35(24%) vs 69 (48%), 36(25%) vs 44(31%), 50(35%) vs 52(36%), 44(31%) vs 45(31%) in the frontal, parietal, temporal, thalamus and basal ganglia respectively. In posterior cerebral territories. The number of hypoperfusion foci in occipital lobe and cerebellum of visual assessment and NeuroGam aided assessment were 18(13%) vs 21 (15%) and 30(21%) vs 35(24%). After the operation, the number of perfusion defects were seen in 49(34%) vs 73(51%), 35(24%) vs 60(42%), 29(20%) vs 35(24%), 16(11%) vs 19 (13%), 47(33%) vs 50(35%), 36(25%) vs 39(27%), 21(15%) vs 29(20%) between visual assessment and NeuroGam combined diagnosis in frontal, parietal, temporal, occipital lobe, thalamus, basal ganglia and cerebellum. Significant differences between visual diagnosis and NeuroGam software aided were seen before and after surgery in different ROI ($P < .0001$) (Tables 1 and 2, image of No. 1 patient in Table 1 was shown in Fig. 1 A–E). Perfusion data analyzed by NeuroGam software before and after revascularization in the same patient were shown in Table 3.

Table 1

Location of foci according to Visual and NeuroGam methods.

No.	Pre-visual-SPECT	Post-visual-SPECT	Pre-NeuroGam-SPECT	Post-NeuroGam-SPECT
1	R Th-Fr	R Th-Bg	R Th-Fr-C	R Th-Bg
2	Bi Fr	Bi Fr	Bi Fr-P	Bi Fr-P
3	R Fr-T, (R Bg-Th)	R Bg	R Fr-T, (R Bg-Th)	R Bg
4	R Bg-Th	R Bg-Th	R Bg-Th-T-C, (Bi Fr)	R P-Fr-O-Bg-Th
5	R Fr	Bi Fr, LP	Bi Fr, L O	Bi Fr, L P
6	L Fr-T-Bg	L Fr-T-Bg	L Fr-T-Bg	L Fr-T-Bg
7	–	R Th-C	–	R Th-C
8	(R T)	R Fr-T	(R T)	R Fr-T
9	–	R Th-C	R Fr	R Fr-T-Th-C
10	R Fr-P-T-O-Bg	R Th-Fr-P	R Fr-P-T-O-Bg	R Th-Fr-P
11	R Fr-P-Th, L C	R Fr-P-Th	R Fr-P-Th, L C	R Fr-P-Th, LC
12	R Fr-P-T-O-Th-Bg, (LC)	R Fr-P-T-O-Th-Bg, (LC)	R Fr-P-T-O-Th-Bg, (LC)	R Fr-P-T-O-Th-Bg, (LC)
13	R O-T-P, (R Bg-Th-C)	R O-T-P, (R Bg-Th-C)	R O-T-P, (R Bg-Th-C)	R O-T-P, (R Bg-Th-C)
14	Bi Fr-P, R C	R Fr, (Bi P, L Fr, R C)	Bi Fr-P, R C	R Fr, (Bi P, L Fr, R C)
15	L Fr-Bg-Th, (R C)	L Fr, (R C)	L Fr-P-T-O-Bg-Th, (R C)	L Fr, (R C)
16	R Fr-T-P-Th, (L C)	R Fr-P-Th-Bg, (L C)	R Fr-T-P-Th, (LC)	R Fr-P-Th-Bg, (L C)
17	R Fr-Th, (L Fr, L C)	L Fr-P	R Fr-Th, (L Fr, L C)	Bi P, L Fr
18	R Fr-P-T-O, (R Bg, L Th)	R P-O	R Fr-P-T-O, (R Bg, L Th)	R P-O
19	Bi Fr	Bi Fr	Bi Fr	Bi Fr
20	R O-T-P-Fr, (R Bg-Th)	R O-T-P-Fr, (R Bg-Th)	R O-T-P-Fr, (R Bg-Th)	R O-T-P-Fr, (R Bg-Th)
21	R Bg	R Bg	R Bg, R Fr-P, (L Fr-P)	Bi Fr-P, R O-Bg, L C
22	Bi O, R P-C	Bi P-O-Th	Bi O, R P-C	Bi P-O-Th, L C
23	–	–	(Bi Fr-P, L Th)	(Bi Fr)
24	R Bg-Th-C	R Bg-Th	R Bg-Th-C	R Fr-P-Bg-Th
25	R Bg-Th	–	R Bg-Th-T-C	–
26	R Fr-P-T-O-Bg-Th	R Fr-P-T-O-Bg-Th	R Fr-P-T-O-Bg-Th	R Fr-P-T-O-Bg-Th
27	R Bg-Th, (R Fr-P-T)	R Fr-P-T-Bg-Th	R Bg-Th, (R Fr-P-T)	R Fr-P-T-Bg-Th
28	R T-Bg-Th, (R Fr-P)	R T-Bg-Th	R T-Bg-Th, (R Fr-P)	R T-Bg-Th
29	L Fr, R T	R T-O-P	L Fr, R T	R T-O-P
30	R Fr-P-T-Bg-Th, L C	Bi Fr, R P-T-Bg-Th, L C	R Fr-P, (L Fr-P, R T-Bg-Th, L C)	Bi Fr, R P-T-Bg-Th, L C
31	L Fr-P-T-Bg-Th, (R C)	L Fr-P-T-Bg, Bi Th, (R C)	L Fr-P-T-Bg-Th, (R C)	L Fr-P-T-Bg, Bi Th, (R C)
32	R Bg-Th	R Th, Bi Fr	R Bg-Th, Bi Fr	R Th, Bi Fr
33	R O, L T, R Th	R O, Bi Fr, L T, R Th	R O, Bi Fr-P, L T, R Th	R O, Bi Fr, L T, R Th
34	R Fr-P-O-T-Bg-Th	R Fr-P-O-T-Bg-Th	Bi Fr-P-T, R Bg-Th-O-C	Bi Fr-P-T, R Bg-Th-O-C
35	L Fr, R Th-Bg	L Fr-P	L Fr, (R Th-Bg, R Fr-P)	L Fr, Bi P
36	–	R T-Th-Bg	Bi Fr-P-T	Bi Fr, R T-Th-Bg, L C
37	R Fr-Bg-Th, L C	R Fr-Th-Bg-P, L C	R Bg-Th, (Bi Fr-P, L C)	R Fr-Th-Bg-P, L C

(*continued*)

Table 1

(continued).

No.	Pre-visual-SPECT	Post-visual-SPECT	Pre-NeuroGam-SPECT	Post-NeuroGam-SPECT
38	L T-P-O, (L C, R Fr-P)	L T-P-O-Bg-Th-C	L T-P-O, (L C, R Fr-P)	L T-P-O-Bg-Th-C
39	L Bg-Th	L Th	L Fr-P-Bg-Th	L Fr-T, (L Th)
40	L Fr-P-T-Th-Bg, R C	L Fr-P-T-Bg-Th, R C	L Fr-P-T-Th-Bg, R C	L Fr-P-T-Bg-Th, R C
41	L Fr-P-T-O-Th-Bg, R C	L Fr-P-T-Th-Bg, R C	L Fr-P-T-O-Th-Bg, R C	L Fr-P-T-Th-Bg, R C
42	L Th, R C	L Th	L Th, R C	L Th
43	R Bg-Th, L T-O	L T	R Bg-Th, L T-O	L Fr-P, (L T)
44	L Th, (L Bg-T)	L Fr, L Bg-Th	L Th, (L Bg-T)	L Fr, (L Bg-Th)
45	L Th-Bg, (R C)	R Fr-P-C	L Th-Bg, (R C)	R Fr-P-C
46	L Bg	L Bg-Th	L Bg	L Bg-Th, (Bi Fr-P)
47	(L Bg-Th)	–	(L Bg-Th)	–
48	L Fr-P-T-O-Bg, R C	L Fr-P-T-O-Bg-Th, R C	L Fr-P-T-O-Bg, R C	L Fr-P-T-O-Bg-Th, R C
49	L Th	L Th	L Th-Bg, (R O-C)	L Th
50	L Th	L Th	Bi Fr-P, L Th	L P-Th, Bi Fr
51	L Fr-Bg-Th, R C	L Th	L Fr-P, (R Fr-P, L C-Bg-Th)	L Fr-P-Th, (R Fr-P, L C)
52	L Th, R C	L Th	Bi Fr-P, L T-Th, R C	L Bg-Th, (R C)
53	L Fr-T-Bg-Th	L Fr-P-Bg-Th	L Fr-T-P-Bg-Th	L Fr-P-Bg-Th
54	L Bg-Th-T-Fr-P, (R C)	L Bg-Th-T-Fr-P, (R C)	L Bg-Th-T-Fr-P, (R C)	L Bg-Th-T-Fr-P, (R C)
55	L Bg-Th	L Fr-P-T-Bg-Th	L Bg-Th, (Bi Fr-P-T)	L Fr-P-T-O-Bg-Th
56	L Fr-Bg-O, R C	L Fr-Bg-Th-O-T-P, R C	L Fr-Bg-Th-O, R C	L Fr-Bg-Th-O-T-P, R C
57	L Fr-P-Bg	Bi Fr, L P-Th-Bg	Bi Fr-P, L Bg	Bi Fr-P, L Th-Bg
58	L Fr-P-T-Bg-Th, (R C)	L Fr-Bg-Th	L Fr-P-T-Bg-Th, (R C)	L Fr-Bg-Th
59	R Bg-Th	Bi T, R Bg	R Bg-Th	Bi T, R Bg
60	L Bg-Th	L Bg-Th	L Bg-Th, Bi Fr	L Fr-Bg-Th, (R Fr)
61	L Fr-P-T-O-C	L Fr-P-T-O-C	L Fr-P-T-O-C, (R Fr-P-T)	L O-C, L Fr-P-Bg-Th-T, (R C)
62	L Bg-Th	L Bg-Th	L Bg-Th, Bi Fr-P	L Bg-Th, Bi Fr-P
63	L Fr-Bg-Th-C, R Fr-P-T	Bi Fr, L Bg-Th-C, R P	L Fr-Bg-Th-C, R Fr-P-T	L P-Bg-T, R Fr-P-T-C-Th
64	L Th, R C	L Th	(L Th, Bi Fr-P, R C)	(L Th, Bi Fr-P-T, R C)
65	L Fr-P-T-O-Bg, (R C)	L Fr-P-T-O-Bg-Th, (R C)	L Fr-P-T-O-Bg, (R C)	L Fr-P-T-O-Bg-Th, (R C)
66	R T-O-P-Fr, (L Fr, R Bg-C)	R Fr-T-O-P, L Fr-Bg, (R C)	R T-O-P-Fr, (L Fr, R Bg-C)	R T-O-P-Fr-Bg-Th, (R C)
67	L Fr-T-P-Bg-Th, (R Fr-P-C)	–	L Fr-T-P-Bg-Th, (R Fr-P-C)	–
68	L Fr-Th	Bi Fr, L P-T	L Fr-P, (L Th, R Fr-P)	L P, Bi Fr, R P, L Th-Bg
69	(Bi Fr-P-T, R Th)	–	(Bi Fr-P-T, R Th)	Bi Fr-P
70	L T-Th	L T	L T, L Th, (Bi Fr)	L T
71	Bi Fr-P-T-Th, R C	–	Bi Fr-P-T-Th, R C	–
72	L P	–	L P	–

() = slightly, - = normal, Bg = basal ganglia, Bi = bilateral, C = cerebellum, Fr = frontal, L = left, O = occipital, P = parietal, Post-NeuroGam-SPECT = hypoperfusion regions found on SPECT/CT images combined visual diagnosis with NeuroGam 3D images after the revascularization surgery, Post-visual-SPECT = hypoperfusion regions found on SPECT/CT images by visual diagnosis after the revascularization surgery, Pre-NeuroGam-SPECT = hypoperfusion regions found on SPECT/CT images combined visual diagnosis with NeuroGam 3D images before the revascularization surgery, Pre-visual-SPECT = hypoperfusion regions found on SPECT/CT images by visual diagnosis before the revascularization surgery, R = right, T = temporal, Th = thalamus.

Crossed cerebellar hypoperfusion (CCH) is a phenomenon of SPECT brain perfusion images that is characterized by reduction in blood flow in the cerebellar hemisphere contralateral to a supratentorial.[16] Among 72 patients, 35 cases of hypoperfusion foci were found in cerebellum before operation by NeuroGam, and 22 cases of them was CCH. After operation, 19 cases of 29 patients who had reduced blood flow in the cerebellum on SPECT imaging was CCH.

Table 2

Results of Visual and NeuroGam methods to assess in bilateral hemisphere foci.

Lobe	Pre-Visual/ NeuroGam-SPECT foci	Post-Visual/ NeuroGam-SPECT foci
Frontal	50/88	49/73
Parietal	35/69	35/60
Temporal	36/44	29/35
Occipital	18/21	16/19
Thalamus	50/52	47/50
Basal Ganglia	44/45	36/39
Cerebellum	30/35	21/29

In the preoperative SPECT/CT combined with NeuroGam study, the mean pixel values of potential surgical hemispheres in corresponding ROI were estimated at the percentage of 52.15 ± 4.71, 55.20 ± 6.30, 50.49 ± 5.15, 63.79 ± 7.90, 46.12 ± 6.94, and 36.90 ± 8.48 in the frontal, parietal, temporal, occipital lobe, thalamus and basal ganglia. And the mean values of contralateral hemispheres were estimated at the percentage of 54.28 ± 4.20, 57.61 ± 4.68, 52.87 ± 3.97, 66.23 ± 6.53, 48.31 ± 5.74, and 38.91 ± 7.98. The mean values of the hemispheres with ischemic events were significantly lower than those of the contralateral hemisphere (paired t test $P < .05$, respectively).

In the follow-up study, the postoperative mean pixel values of surgical hemisphere were 53.54 ± 4.78, 56.74 ± 5.81, 52.48 ± 4.96, 64.58 ± 7.42, 45.42 ± 6.59, and 38.45 ± 8.84 in the frontal, parietal, temporal, occipital lobe, thalamus and basal ganglia. However, the mean values of unsurgical hemisphere were 55.12 ± 3.92, 58.41 ± 4.80, 53.74 ± 4.26, 66.24 ± 6.80, 48.16 ± 5.75, and 38.85 ± 7.80 in those regions (paired t test, $P = .002$, .007, .024,

Table 3

Perfusion data were analyzed by NeuroGam software before and after revascularization in the same patient.

Values	Frontal	Parietal	Temporal	Occipital	Thalamus	Basal ganglia	Cerebellum
Pre-surgical hemisphere	53.2	56.6	51.1	70.6	34.4	28.3	57.6
Post-7 days surgical hemisphere	53.8	57.4	51.9	67.9	37.4	38.8	50
Post-7 months surgical hemisphere	55.7	58.9	55.2	69.8	31.7	26.9	53.6
Pre-unsurgical hemisphere	55	59.3	53.5	67.3	42.7	27.1	57.3
Post-7 days unsurgical hemisphere	55.6	57.7	52.7	65.3	42.1	27.8	50.2
Post-7 months unsurgical hemisphere	57.5	60.5	56.1	66	48.5	33.5	51.4

.158, .000, .680, respectively). Differences between pre- and post-operation were found in the frontal lobe ($t=-3.734$, $P=.000$), the parietal lobe ($t=-3.935$, $P=.000$) and the temporal lobe ($t=-5.099$, $P=.000$) according to NeuroGam software. However, no significant differences were found in the occipital lobe ($t=-1.962$, $P=.054$), thalamus ($t=1.362$, $P=.177$), basal ganglia ($t=-2.394$, $P=.019$) and cerebellum ($t=1.383$, $P=.171$) (Fig. 2). Preoperative brain perfusions SPECT in patients of surgical side were significantly different from those of contralateral side ($P<.05$). Postoperative brain perfusions of anterior and middle cerebral regions of surgical side were significantly improved. However, no significant differences were found in posterior cerebral circulation regions and basal ganglia after surgical revascularization ($P>.05$).

Perfusion changes were found visually by comparison with contralateral brain parenchyma. Before STA-MCA+EDMS, cerebral hypoperfusion was found in all 72 patients, and 30 of them had normal CT or MRI. After STA-MCA+EDMS, the following changes of perfusion could observe by 3D of NeuroGam software. Twenty-nine patients had elevated perfusion (ipsilateral and bilateral), while 15 had deterioration and 28 remained no change.

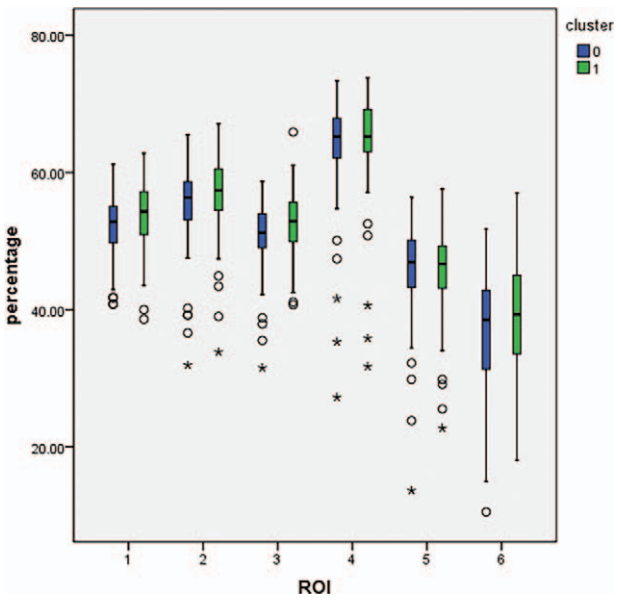

Figure 2. NeuroGam software analyzed mean percentage of the whole brain perfusion between pre- and post-operation. Note: 0Blue represents mean percentage of the whole brain perfusion with NeuroGam before the revascularization surgery; 1green represents mean percentage of the whole brain perfusion with NeuroGam after the revascularization surgery; 1, frontal lobe; 2, parietal lobe; 3, temporal lobe; 4, occipital lobe; 5, thalamus; 6, caudate nucleus.

4. Discussion

Our report describes patients suffering from insufficient cerebral blood flow could benefit from cerebral revascularization surgery. Quantitative SPECT/CT combined with NeuroGam software provides objective assessment of cerebral perfusion of impaired cortices and cerebellar ganglia.

SPECT brain perfusion imaging is a reliable method to reflect cortical function.[9] In previous studies, traditional visual inspection lacks objective indexes when comparing longitudinal SPECT/CT brain images. Nowadays, several computer aided approaches have been applied to image processing to quantify cortical perfusion.[17] The NeuroGam software is one of the statistical analysis tools for automated diagnosis of brain perfusion on SPECT brain perfusion images. It applies an affine anatomical co-registration template for brain standardization.[18,19] Using this software could help identify the impaired perfusion regional earlier by means of quantitative comparison. Moreover, it could display brain perfusion data through visual inspection in a 3D anatomical topographic which represented in different colors.[20] The NeuroGam software analysis tools diagnose the brain perfusion by comparing with template of brain standardization automatically. Therefore, even the person who does not understand nuclear medicine imaging could obtain a general understanding of abnormal perfusion regions.

In our study, the radionuclide imaging of SPECT with $^{99m}T_C$-ECD was used in conjunction with a voxel-based analysis named NeuroGam to quantify the cerebral blood perfusion in 72 patients with MMD before and after the STA-MCA+EDMS cerebral revascularization. As a result, we found that the patients showed hypoperfusion in potential surgical hemisphere. However, most of them had increased cerebral blood perfusion in anterior cerebral regions of the surgical hemisphere, particularly in the frontal, parietal, temporal lobe. Brain perfusion in these areas were marked highly than pre-operation (Fig. 2). Meanwhile, the patients showed no change or deteriorate cerebral blood perfusion in posterior regions and basal ganglia, primary in the occipital lobe, cerebellum, thalamus and caudate nucleus. Previous studies described the surgery experience of STA-MCA +EDMS for MMD, and found significant improvement of cerebral perfusion in both the middle cerebral artery and anterior cerebral artery territories after surgery. The result may due to the characteristics of indirect revascularization which can effectively improve the blood supply of anterior circulation, but not the posterior circulation.[21]

The low dose, non-contrast CT is acquired in conjunction with the SPECT study to produce the fused SPECT/CT image. Combined with CT, SPECT/CT hybrid cameras provides more morphologic precision than only functional specificity. It makes SPECT/CT an ideal technique for postsurgical patients. The most

important role of CT in the examination of the brain perfusion is not the fusion of the perfusion image and morphological image but enabling accurate attenuation correction.[22]

Prior reports were based on SPECT with acetazolamide challenge using quantitative CBF, perfusion weighted magnetic resonance imaging (MRI)[23] and positron emission tomography (PET). SPECT has been used to demonstrate hypoperfusion of bilateral frontal medial cortices in patients with MMD. According to previous findings of Young So et al,[9] basal/acetazolamide stress brain perfusion SPECT performed after the operation could predict the further clinical outcome of pediatric patients with MMD. Patients who had decreased cerebrovascular reserve showed the worst postoperative clinical outcomes. Recent studies using ^{123}I iomazenil (IMZ-SPECT) to investigate the relationship between higher brain dysfunction and cortical neuron loss in patients with MMD.[24] Whereas acetazolamide test about cerebral blood flow measurement are complicated procedures with some uncontrolled risk, which makes it difficult to apply in routine clinical examination. In an earlier SPECT study, a non-invasive calculation of regional absolute CBF using $^{99m}T_C$-ECD was reported, which combined with application of a linearization algorithm.[25]

A previous study showed that perfusion MRI with some kinds of special sequences, such as ADC could measure executive dysfunction in patients with MMD.[26] PET also was used to investigate metabolism and the effect of bypass surgery. And the results showed that preoperative regional cerebral blood flow (rCBF) and regional cerebral metabolic rate of oxygen (rCMRO2) decreased while the regional oxygen extraction fraction (rOEF), the regional cerebral blood volume (rCBV) and mean transit time (MTT) were significantly increased.[27,28] A prospective observational study hypothesized that the increased OEF was an independent predictor of stroke in patients with MMD.[29] Although PET seemed to be the most accurate, the complication and huge cost limited its application.

Surgical techniques were confirmed to improve cerebral perfusion, especially direct (STA-MCA) bypass could provide immediate augmentation of blood flow.[30] Neurologic deficit and transient ischemic attacks are expected to be solved after successful bypass surgery. Calviere et al[31] found improvement of cognitive impairment after revascularization located in frontal areas in an adult with MMD. Since the functional areas of these perfusion changes correspond to the clinical features in patients with MMD, we believe that the regional perfusion measurements in this study might be useful to predict clinical outcome in MMD. Furthermore, early diagnosis and wider range of revascularization procedure may be essential to improve their intellectual outcomes.[4]

To the best of our knowledge, direct correlation between these parameters has not been reported before. Our results were based on a more accurate quantitative method (voxel-based), which in accordance with the findings of Paschali et al that NeuroGam software could quantify perfusion images of each patient comparing with a normative database.[15] Therefore, the data presented in our study are novel. What is more, we found that the parietal lobe had been posed as a crucial factor added to frontal lobe in MMD patients. Some of the patients in our study also exhibited significant hypoperfusion of the parietal lobe which further showed significant correlations with low performance. Our findings corroborate previous reports regarding redistribution of perfusion after surgery.[32–33]

Postoperative hyperperfusion is the most serious complication in MMD patients after revascularization surgery, and extreme procedural care is postulated in patients at risk. Postoperative hypoperfusion may due to hard to anastomosis, surgical trauma, collateral formation has been destroyed.[34] However, no such case was found in our study.

In our opinion, NeuroGam software may be useful in clinical practice. It can be easily and quickly obtained from brain perfusion SPECT, which is a noninvasive diagnostic method and is relatively inexpensive. When comes semi-quantitative perfusion evaluation, most studies have used ROI approaches. These methods are operator-dependent, time-consuming, and the analysis cannot cover the entire brain cortices. This new image processing is automatic and 3-dimensional method, which provides a faster and more objective assessment of the whole brain. Besides, there is no difficult comparing baseline and control SPECT image because the voxel-based approach guarantees accuracy of obtained results. However, for the lack of MRI image database, we could not use MRI data to provide the anatomical reference.

There are still some limitations in our study. First, the radiation to the brain by SPECT/CT is unavoidable. Second, due to the chronic course of MMD, researches regarding long-term outcomes as well as further understanding of the brain perfusion are needed. Third, more attention should be paid on correlation analysis between regional cerebral hemodynamics and neuropsychological functioning in patients with MMD. Fourth, assessment of vessel reserve with acetazolamide is often an important part of brain perfusion imaging in cerebrovascular disease. Lack of this test is also a limitation of the present study.

In conclusion, NeuroGam software provides a quantitative approach for monitoring surgical effect of MMD in a variable time (3–12 months after surgery). It could discover the perfusion changes that are neglected in conventional visual assessment.

Author contributions

Conceptualization: Jingjing Lou, Bin Xu, Xingdang Liu.
Data curation: Jingjing Lou, Bin Xu, Yuankai Wang, Congjin Liu, Miao Liu.
Formal analysis: Congjin Liu.
Methodology: Zhuang Liu.
Resources: Zhuang Liu, Xingdang Liu.
Software: Yuankai Wang, Congjin Liu.
Supervision: Bin Xu, Xingdang Liu.
Writing – original draft: Zhuang Liu.
Writing – review & editing: Xingdang Liu.

References

[1] Suzuki J, Takaku A. Cerebrovascular "moyamoya" disease. Disease showing abnormal net-like vessels in base of brain. Arch Neurol 1969;20:288–99.
[2] Kuroda S, Houkin K. Moyamoya disease: current concepts and future perspectives. Lancet Neurol 2008;7:1056–66.
[3] Kuroda S, Hashimoto N, Yoshimoto T. Radiological findings, clinical course, and outcome in asymptomatic moyamoya disease: results of multicenter survey in Japan. Stroke 2007;38:1430–5.
[4] Kuroda S, Houkin K, Ishikawa T, et al. Determinants of intellectual outcome after surgical revascularization in pediatric moyamoya disease: a multivariate analysis. Childs Nerv Syst 2004;20:302–8.
[5] Fukui M. Guidelines for the diagnosis and treatment of spontaneous occlusion of the circle of Willis (Moyamoya' disease). Clin Neurol Neurosurg 1997;99:S238–40.

[6] Guzman R, Lee MA. Clinical outcome after 450 revascularization procedures for moyamoya disease. Clinical article. J Neurosurg 2009;111:927–35.
[7] Saito N, Nakagawara J, Nakamura H, et al. Assessment of cerebral hemodynamics in childhood moyamoya disease using a quantitative and a semiquantitative IMP-SPECT study. Ann Nucl Med 2004;18:323–31.
[8] Ramon N, Kevin C, Gooderham PA, et al. Less-invasive pedicled omental-cranial transposition in pediatric patients with moyamoya disease and failed prior revascularization. Neurosurgery 2014;10:1–4.
[9] So Y, Lee HY, Kim SK, et al. Prediction of the clinical outcome of pediatric moyamoya disease with postoperative basal/acetazolamide stress brain perfusion SPECT after revascularization surgery. Stroke 2005;36:1485–9.
[10] Noguchi T, Kawashima M, Irie H, et al. Arterial spin-labeling MR imaging in moyamoya disease compared with SPECT imaging. Eur J Radiol 2011;80:e557–62.
[11] Kong B, Zhan Y, Shin M, et al. Recognizing end-diastole and end-systole frames via deep temporal regression network. MICCAI 2016;264–72.
[12] Carrillo Mezo R, Lara Garcia J, Arroyo M, et al. Relevance of 3D magnetic resonance imaging sequences in diagnosing basal subarachnoid neurocysticercosis. Acta Trop 2015;152:60–5.
[13] Xu B, Song DL, Mao Y, et al. Superficial temporal artery-middle cerebral artery bypass combined with encephalo-duro-myo-synangiosis in treating moyamoya disease: surgical techniques, indications and midterm follow-up results. Chinese Med J 2012;125:4398–405.
[14] Juni JE, Waxman AD, Devous , et al. Procedure guideline for brain perfusion SPECT using 99mTc radiopharmaceuticals 3.0. J Nucl Med Tech 2009;37:191–5.
[15] Paschali A, Messinis L, Kargiotis O, et al. SPECT neuroimaging and neuropsychological functions in different stages of Parkinson's disease. Euro J Nucl Med Mol Im 2010;37:1128–40.
[16] Komaba Y, Mishina M, Utsumi K, et al. Crossed cerebellar diaschisis in patients with cortical infarction: logistic regression analysis to control for confounding effects. Stroke 2004;35:472–6.
[17] Sun WB, Ruan Zet, Dai X, et al. Quantifying hemodynamics changes in moyamoya disease based on 2D cine phase-contrast MRI and computational fluid dynamics. World Neurosurg 2018;120:E1301–9.
[18] Paschali A, Mwssinis L, Karfiotis O, et al. SPECT neuroimaging and neuropsychological functions in different stages of Parkinson's disease. Eur J Nucl Med Mol Im 2010;37:1128–40.
[19] Valotassiou V, Sifakis N, Zerva C, et al. Evaluation of brain perfusion in specific Brodmann areas in Frontotemporal dementia and Alzheimer disease using automated 3-D voxel based analysis. J Instrum 2009;4:05020.
[20] Selva-O'Callaghan A, Bardes I, Jacas C, et al. SPECT imaging for brain improvement quantification in a patient with cerebrotendinous xanthomatosis. Clin Nucl Med 2011;36:38–9.
[21] Kuroda S, Houkin K, Ishikawa T, et al. Novel bypass surgery for moyamoya disease using pericranial flap: its impacts on cerebral hemodynamics and long-term outcome. Neurosurgery 2010;66:1093–101.
[22] Ishii K, Hanaoka K, Okada M, et al. Impact of CT attenuation correction by SPECT/CT in brain perfusion images. Ann Nucl Med 2012;26:241–7.
[23] Nakamizo A, Kikkawa Y, Hiwatashi A, et al. Executive function and diffusion in frontal white matter of adults with moyamoya disease. J Stroke Cerebrovasc Dis 2014;23:457–61.
[24] Nakagawara J, Osato T, Kamiyama K, et al. Diagnostic imaging of higher brain dysfunction in patients with adult moyamoya disease using statistical imaging analysis for [123I]iomazenil single photon emission computed tomography. Neurol Med Chir (Tokyo) 2012;52:318–26.
[25] Laere KV, Dumont F, Koole M, et al. Non-invasive methods for absolute cerebral blood flow measurement using 99mTc-ECD: a study in healthy volunteers. Eur J Nucl Med 2001;28:862–72.
[26] Tanaka Y, Nariai T, Nagaoka T, et al. Quantitative evaluation of cerebral hemodynamics in patients with moyamoya disease by dynamic susceptibility contrast magnetic resonance imaging—comparison with positron emission tomography. J Cerebr Blood F Met 2005;26:291–300.
[27] Ikezaki K, Matsushima T, Kuwabara Y, et al. Cerebral circulation and oxygen metabolism in childhood moyamoya disease: a perioperative positron emission tomography study. J Neurosurg 1994;81:843–50.
[28] Nariai T. Severe haemodynamic stress in selected subtypes of patients with moyamoya disease: a positron emission tomography study. J Neurol Neurosurg Psychiatry 2005;76:663–9.
[29] Zipfel GJ, Sagar J, Miller JP, et al. Cerebral hemodynamics as a predictor of stroke in adult patients with moyamoya disease: a prospective observational study. Neurosurg Focus 2009;26:E6.
[30] Khan N, Schuknecht B, Boltshauser E, et al. Moyamoya disease and Moyamoya syndrome: experience in Europe; choice of revascularisation procedures. Acta Neurochir (Wien) 2003;145:1061–71.
[31] Calviere L, Catalaa I, Marlats , et al. Improvement in cognitive function and cerebral perfusion after bur hole surgery in an adult with moyamoya disease. Case report. J Neurosurg 2011;115:347–9.
[32] Duan L, Bao X-Y, Yang W-Z, et al. Moyamoya disease in China: its clinical features and outcomes. Stroke 2012;43:56–60.
[33] Funaki T, Takahashi JC, Takagi Y, et al. Incidence of late cerebrovascular events after direct bypass among children with moyamoya disease: a descriptive longitudinal study at a single center. Acta Neurochir 2014;156:551–9.
[34] Zhang J, Wang J, Geng D, et al. Whole-brain CT perfusion and CT angiography assessment of moyamoya disease before and after surgical revascularization: preliminary study with 256-slice CT. PloS One 2013;8:e57595.